Improved Impact-Echo Approach for Non-Destructive Testing and Evaluation

R. ZHANG, L.D. OLSON, and A. SEIBI, A. HELAL, A.KHALIL, M. RAHIM
Division of Engineering, Colorado School of Mines, Colorado USA,
Olson Engineering, Inc., Colorado, USA and
Department of Mechanical Engineering, Petroleum Institute, Abu Dhabi, UAE
rzhang@mines.edu http://engineering.mines.edu/undergraduate-program/civil-engineering/faculty/detail/?fid=62

Abstract: This study examines rationale of correction factor β in the formula of thickness resonant frequency, fundamental to the impact-echo (IE) approach in non-destructive testing and evaluation for integrity appraisal and damage diagnosis of infrastructure systems. It shows the role of the factor in the resonant frequency which is typically obtained with average characteristic from traditional fast Fourier transform or FFT data analysis of IE recordings. A time-frequency data analysis termed Hilbert-Huang Transform or HHT is then introduced to overcome the shortage of FFT analysis in identifying the resonant frequency from IE recordings. With the FFT and HHT analyses of five data sets of sample IE recordings from sound and damaged concrete structures and comparison with referenced ones, this study reveals that the proposed IE approach with HHT data analysis not only eliminates the use of correction factor in the formula, it also improves greatly the accuracy in the IE approach.

Key-Words: Impact-Echo, Non-Destructive Testing and Evaluation, Hilbert-Huang Transform

1 Introduction

Impact-echo (IE) approach of non-destructive testing (NDT) is widely used for non-destructive evaluation (NDE) of integrity and damage of various concrete and steel structures, exemplified as building beams/columns/walls, bridge decks, tunnel walls, post-tensioned ducts, pavements, and pipes. As schematically shown in Fig.1, the elastic impact of a steel sphere on a tested or working surface of a structure generates longitudinal waves, which travel back and forth between the working and other side of the structure or internal face of defects like crack, delamination or void. Analysis of the wave echo signals received at the position next to the impact location in general, and finding the resonant frequency with FFT data analysis in particular, helps determine the depth of the structure or depth to the defect, which can help evaluate the structural integrity and diagnose internal damage.

The fundamental to the IE approach is based on one-dimensional wave propagation theory or formula for the thickness resonant frequency f [1-2]

$$f = \frac{\beta c}{h} \tag{1}$$

where h is the thickness of the structure or thickness to the defect, c the longitudinal or P-wave speed, and β the empirical correction factor accounting for the shape of the structure when it was first introduced, which takes 0.96 for plate structures [1] and ranges from 0.87 to 0.96 dependent upon the size of the structure [3], among others.

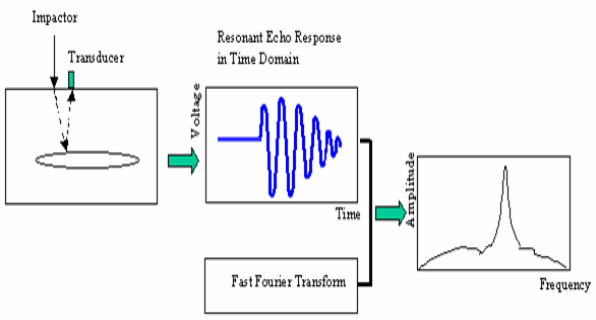

Fig. 1: Schematic of impact-echo approach in NDT/E (courtesy of L. Olson)

Equation (1) implies that the thickness is typically overestimated with a given P-wave speed and measured resonant frequency from wave echo recording if no correction factor is considered or β=1. Recent studies [3-6] attribute the overestimation or correction factor to wave scattering and/or dispersion features resulted from two- or three-dimensional wave propagation in the structure with a finite size and different boundaries. While the aforementioned studies, together with many others, advance the understanding of the role of correction factor in Eq. (1) and subsequently improve accuracy for thickness estimation, the perspective for correction factor is limited and

suggested values to be used in the IE approach is subjective. This paper in the following sections tries to examine broadly the cause of the overestimation and propose an alternative way to eliminate the use of the subjective correction factor, while still improving accuracy of the IE for NDT/E.

2 Physics of Correction Factor

Examining any kind of IE equipments, exemplified as simple CTG (Concrete Thickness Gauge) and comprehensive NDE360 of Olson Instruments, Inc., suggests that the impact position (impactor in Fig. 1) has a non-negligible distance away from the wave-signal receiver (transducer in Fig. 1) on the working surface in comparison with the thickness to be estimated. This indicates that the echoed P-waves received are not travelling back and forth along the thickness h, but a slightly larger $h'= h/\beta_h$ with correction factor for thickness $\beta_h<1$.

Because of the impact-to-receiver surface distance, the problem at hand should be tackled at least within the framework of two-dimensional, in-plane wave propagation in which both P-waves and shear or S-waves are coupled at free, fixed, and/or continuity boundaries, showing wave scattering phenomena in reflection and refraction or reflected and transmitted P- and S-waves from incident P-waves (or S-waves). This yields the echoed waves at the receiver not solely from P-waves, but also from S waves. Considering the non-perfectly-vertical direction of the impactor and transducer to the working surface, one can expect the echoed wave signals at the receiver contain non-negligible S-wave signals in comparison with the P-waves. The mixed P- and S-wave echo will alter the period or frequency of pure P-wave echo shown in the recording, although the effect might be minor. With the fact that S-wave speed is smaller than the P-wave one, all the above suggests that use of P-wave speed in Eq. (1) provides the upper-bound solution for the thickness estimation. At this junction, a realistic smaller wave speed should be used in Eq. (1), i.e., $c'= \beta_c c$ with correction factor for wave speed $\beta_c<1$.

It is of interest to note that surface waves and wave scattering due to the structural finite size and boundaries should not play a major role in the correction factor, while the influence of wave dispersion features needs further quantitative study, which is elaborated below. First, the impact-to-receiver surface distance is so small such that surface waves like non-dispersive Rayleigh (along a free surface) and Stoneley (along a two-layer boundary) waves are not well developed. Second, the geometrical and material damping makes the intensity of wave signals reflected from the boundaries in the non-thickness directions much smaller than that of waves echoed from the thickness direction, for the distance of the receiver to the former boundaries is typically much larger than that to the latter. Third, dispersive wave features may influence the correction factor only when Eq. (1) is used for estimating the thickness to the internal defect, which is strongly dependent upon type/size and direction of the defect relative to the structural thickness and surface horizontal direction respectively.

With fast Fourier transform or FFT of displacement response recording at IE receiver, the resonance frequency in Eq. (1) is typically identified as the dominant frequency with locally-maximum Fourier amplitude in Fourier amplitude spectrum of the recording. Fourier amplitude at a given frequency is associated with harmonic component defined globally over the entire time duration of the recording under investigation and thus meaningful only for stationary data analysis. For the recording at hand which is apparently nonstationary due to different arrivals of P- and S-waves and surface waves, and wave scattering and dispersion, the dominant frequency obtained with FFT essentially gives average, not true, characteristic of resonant frequency over the entire duration of the recording. While the use of short-time or windowed Fourier transform may possibly minimize the nonstationarity in the data caused by different types of wave echo, it cannot resolve the issues of nonstationarity rooted in the wave dispersion. In addition, windowed FFT, or selection of window length for FFT in particular, is subjective. To this end, a modified resonant frequency should be used in Eq. (1), i.e., $f'=f/\beta_f$ with β_f denoting correction factor for resonant frequency that is compensated for FFT-based average frequency identification.

With the aforementioned understanding, correction factor β used in Eq. (1) can be regarded as one combining those three, i.e., $\beta = \beta_h\beta_c\beta_f$.

In principle, thickness can be estimated with improved accuracy if the correction factor is given. In practice, it is almost impossible for having the correction factor corresponding to different shape, size, and boundaries of structure and defects under NDT/E. Nevertheless, recognizing that the influence of correction factors for thickness and wave speed has been implicitly shown in the resonant frequency of the recording, and the resonant frequency changes slightly from time to time in the entire duration of nonstationary

recording, one can use time-frequency data analysis for exploring true resonant frequency and thus abandon the use of correction factor, which is detailed below.

3 Time-Frequency Data Analysis

Alternative to the FFT data analysis, this study proposes the use of a time-frequency data analysis for nonstationary recording [7-8], referred to as Hilbert-Huang transform (HHT), to depict nonstationary features from IE recordings.

The HHT method consists of empirical mode decomposition (EMD) and Hilbert spectral analysis (HSA). Any complicated time domain record can be decomposed via EMD into a finite, often small, number of intrinsic mode functions (IMF) that admit a well-behaved Hilbert transform. The IMF is defined by the following conditions: (1) over the entire time series, the number of extrema and the number of zero-crossings must be equal or differ at most by one, and (2) the mean value of the envelope defined by the local maxima and the envelope defined by the local minima is zero at any point. An IMF represents a simple oscillatory mode similar to a sinusoidal component in FFT analysis, but more general.

The EMD explores temporal variation in the characteristic time scale of the data and thus is adaptive to nonstationary data processes. It functions as a dyadic filter for broad-band noise data [9]. The HSA defines an instantaneous or time-dependent frequency of the data via Hilbert transformation of each IMF component.

The HHT representation of IE recording $X(t)$ is

$$X(t) = \Re\sum_{j=1}^{n} a_j(t)e^{i\theta_j(t)} = \Re\sum_{j=1}^{n}[C_j(t) + iY_j(t)] \quad (2)$$

where $C_j(t)$ and $Y_j(t)$ are respectively the jth IMF component of $X(t)$ and its Hilbert transform $Y_j(t) = \frac{1}{\pi} P\int \frac{C_j(t')}{t-t'}dt'$ with P denoting the Cauchy principal value, and the time-dependent amplitudes $a_j(t)$ and phases $\theta_j(t)$ are the polar-coordinate expression of Cartesian-coordinate expression of $C_j(t)$ and $Y_j(t)$, from which the instantaneous frequency is defined as $\omega_j(t) = d\theta_j(t)/dt$. The Hilbert amplitude spectrum $H(\omega,t)$ and marginal Hilbert amplitude spectrum $h(\omega)$ over time duration T of the data are defined as

$$H(\omega,t) = \sum_{j=1}^{n} a_j(t), \quad h(\omega) = \int_0^T H(\omega,t)dt \quad (3,4)$$

While the Hilbert and marginal Hilbert amplitude spectra provide information similar to the Fourier amplitude spectrum obtained from short-time Fourier transform, its frequency term is different. Fourier-based frequency is constant over the harmonic function persisting through the data window, while HHT-based frequency varies with time. As the Fourier transformation window length reduces to zero, the Fourier-based frequency approaches the HHT-based frequency. Fourier-based frequency is, however, locally averaged and not truly instantaneous for it depends on the window length. Because of the aforementioned unique HHT features, the dominant frequency identified from marginal Hilbert amplitude spectrum is expected closer to the true resonant frequency than that from Fourier amplitude spectrum.

While the broad-based applications of the HHT in time-frequency data analysis in general, and some advantages over FFT in particular, can be found in [10-11] and [12-17] respectively, among many others, most data analyzed are broad-band. In other words, HHT analysis of narrow-band data such as IE recordings is rarely seen. This is likely due to the drawback of EMD for narrow-band data process, i.e., lack of some frequency-band contents or equivalently characteristic time scales in recordings may sometimes make the EMD to mix two widely-separate scale signals into one IMF or difficult to distinguish the two from one IMF, which is called mode mixing issue. To enable the EMD work for narrow-band data in all the cases, a simple, yet proved to be sound and effective, way is to add a finite-amplitude, white noise into the original data [9,18]. The noise-added data is by nature broad-band without change of the frequency distribution, which prepares the HHT analysis effectively for revealing quantifies like resonant frequency from marginal Hilbert amplitude spectrum.

4 Validation with IE Recordings

To illustrate the proposed IE approach with modified data analysis, this study examines five sets of IE recordings for sound and damaged concrete plate structures, provided by Olson Engineering, Inc. The P-wave speed for all the five samples is 12,000 ft/s, and the thicknesses of the sample structures are listed in Table 1, in which samples 3 and 4 have internal defects corresponding to the shorter thicknesses. These thicknesses could be estimated

based on Eq. (1) as well as Fourier-based data analyses such as high-pass filter, smoothing windows and resonant frequency identification. Since the thicknesses of sample structures can be easily validated with direct measurements, all the data listed in Table 1 may reasonably be regarded as referenced, correct thicknesses.

For comparison of IE approach with FFT and HHT data analyses, Eq. (1) without correction factor and unprocessed, raw recordings are used. Figure 2 shows the raw recording of sample 4, which contains significant energy in low-frequency band, resulting from pushing down the IE equipment like CTG in testing for better contact between IE equipment and working surface, dominant wave echo signals in the middle-frequency band, as well as few others like noise in high-frequency band which are not easily observed from the time history. To facilitate the HHT analysis, a white noise is added into the raw recording, in which the white noise power is selected as 10% of original raw one. After performing FFT of raw recordings and HHT of noise-added ones, Fourier amplitude spectra and marginal Hilbert amplitude spectra can be found. Figures 3 and 4 shows respectively the Fourier and marginal Hilbert amplitude spectra of sample 4, from which the marked dominant frequencies can be identified as 7347, 7533, 7719 and 8836 Hz for FFT and 7563 and 8815 Hz for HHT. Note that the frequency scales in Figs. 3 and 4 are different, i.e., the former is linear and the latter is logarithmic. With the use of Eq. (1), the pertinent thicknesses can be found in Tables 2 and 3, in which relative errors with referenced thicknesses are also calculated.

Comparison of Tables 2 and 3 indicates clearly the improved accuracy with HHT analysis over the traditional FFT analysis, which can be elaborated below. First, the relative errors for estimating all the thicknesses are significantly reduced with the HHT analysis from those with traditional FFT analysis, indicating the significant improvement of accuracy for thickness estimation. Second, the HHT analysis can identify uniquely defect-related resonant frequencies and subsequently the pertinent thicknesses, while the FFT sometimes provides multiple peaks in Fourier spectrum as shown in Fig. 3, resulting in multiple resonant frequencies and thicknesses. Third and most important, the thickness estimation with FFT is higher than the referenced one in each and every sample, suggesting that the dominant frequency identified with FFT (f') should be larger than the resonant frequency (f) used in Eq. (1), or $f'= f/\beta$ with $\beta<1$. In other words, correction factor β can be explained as compensation for the inaccurate FFT-based identification of resonant frequency, alternative to the correction for structural shape as introduced in Eq. (1) in the early stage. Note again that the influence of correction factors for thickness and wave speed are not taken into account, for that is inherited in the recording under investigation, or equivalently the resonant frequency identified from the recording should genetically account for the influence of those two factors. Since the HHT analysis can explore the resonant frequency more truthfully than the FFT one, the correction factor is not necessarily used for estimating thickness with Eq. (1).

Table 1: Referenced thicknesses of five sample concrete structures, in which the smaller number in samples 3 and 4 is the thickness related to the internal defects.

Sample No.	Referenced Thickness in *in*.	
1	10.6	
2	10.4	
3	16.2	6.1
4	10.1	8.5
5	10.8	

Table 2: Estimated thicknesses and calculated relative errors with FFT analysis

Sample No.	FFT-based Thickness in *in* (Relative Error in %)				
1	10.87 (2.5)				
2	10.59 (1.8)				
3	16.5 (1.8)	14.0 (13.6)	6.5 (5.8)	6.4 (4.1)	6.3 (2.5)
4	10.5 (4.0)	10.2 (1.0)	9.9 (1.5)	8.7 (2.3)	
5	11.16 (3.3)				

Table 3: Estimated thicknesses and calculated relative errors with HHT analysis

Sample No.	HHT-based Thickness in *in* (Relative Error in %)	
1	10.73 (1.23)	
2	10.43 (0.29)	
3	16.29 (0.56)	6.18 (1.31)
4	10.15 (0.50)	9.58 (0.14)
5	11.00 (1.85)	

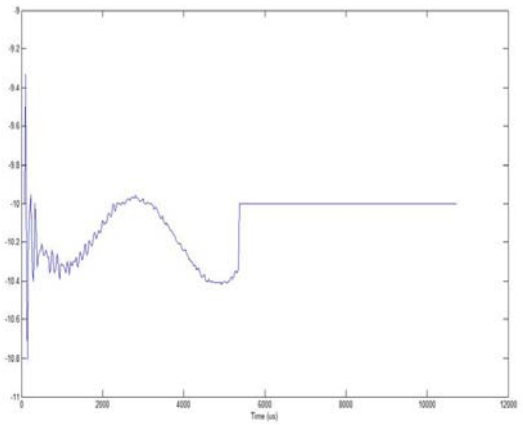

Fig. 2: Unprocessed, raw displacement time-history recording for sample 4.

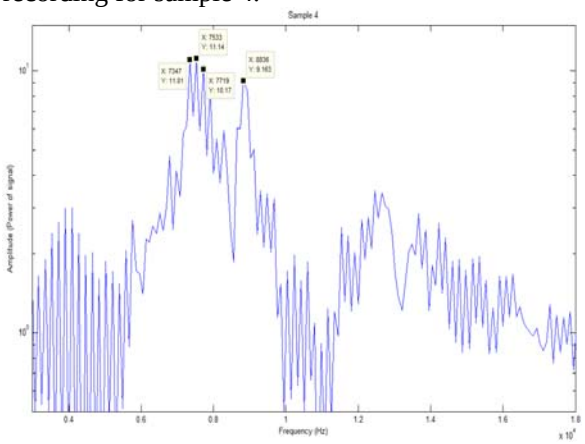

Fig. 3: Frequency amplitude spectrum of displacement response for sample 4, in which marks at some peaks are related to the resonant frequencies used in Eq. (1), and amplitude is in logarithmic scale and frequency in linear one.

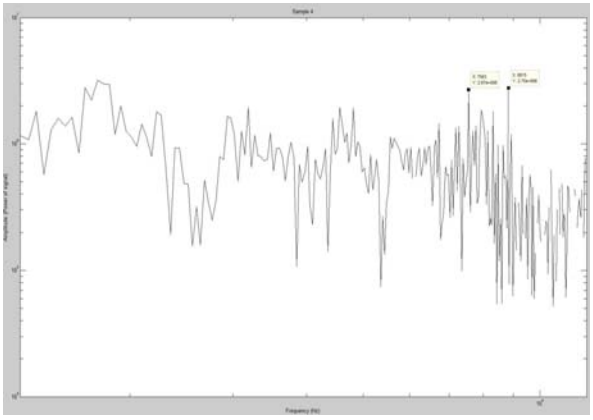

Fig. 4: Marginal Hilbert amplitude spectrum of noise-added displacement response for sample 4, in which marks at some peaks are related to the resonant frequencies used in Eq. (1), and both amplitude and frequency are in logarithmic scale.

5 Concluding Remarks

This study re-examines rationale of the thickness resonant frequency formula, which is based on one-dimensional, longitudinal wave propagation theory and widely used for evaluating integrity and damage of structures with an IE approach. The investigation addresses the multiple influences of the two-dimensional wave propagation and resonant frequency identification in the formula in general and correction factor in particular. It is found that the correction factor used in the formula should not be designated for influence of the structural shape. Instead, it combines influences of measurement of dominant frequency for data analysis, dominant wave propagation path, wave scattering and dispersion due to the boundary conditions in structure and defects. After detailing the limitation of traditional FFT data analysis in exploring resonant frequency, this study proposed the use of time-frequency HHT analysis of noise-added recordings. Numerical examples of five sets of raw IE recordings from sound and damaged structures show not only the significantly-improved accuracy in estimating the thickness with proposed IE approach, but also demonstrate that the correction factor can be dropped out from the thickness resonant frequency formula.

It should be pointed out that the results from this study are based on qualitative analysis of thickness resonant frequency formula and verified with a limited number of IE recordings. They must, therefore, be validated further by model-based simulation and recordings-supply analysis.

While the proposed HHT analysis of noise-added recordings does improve the thickness estimation accuracy, other alternative approaches may equivalently do the same or further advances it. One is the use of Hilbert transform analysis of recordings instead of HHT, if the recordings admit a well-behaved Hilbert transform, i.e., no non-physical instantaneous frequency was withdrawn from the Hilbert transform. Readers are referred to [7-8] for detail. The other is to perform the statistical analysis of IMFs of EMD for noise-added recordings, for the realizations of each and every white noise will be cancelled out in calculating the ensemble average of IMFs, leaving the true IMFs pertinent to the original recording. The theory and advantage of this statistical data process, termed as ensemble EMD or EEMD can be found in [18]. The aforementioned two are subjective to further studies.

6 Acknowledgment

The authors would like to express their sincere gratitude to P. Miller of Olson Engineering, Inc. for supplying IE recordings. This work was partially conducted when the first author took a sabbatical leave from Colorado School of Mines (CSM) and guided senior design projects I and II in mechanical engineering program in Petroleum Institute (PI), Abu Dhabi, United Arab Emirates in 2009-2010. This work was supported by CSM–PI joint research project under the auspices of Abu Dhabi National Oil Company. The opinions, findings and conclusions expressed herein are those of the authors and do not necessarily reflect the views of the sponsors.

References:

[1] Sansalone M.. and W. Streett, *Impact-Echo Nondestructive Evaluation of Concrete and Masonry*, Ithaca, NY: Bullbrier Press, 1997.

[2] ASTM C 1383, Test method for measuring the P-wave speed and the thickness of concrete plates using the impact-echo method, *2000 Annual book of ASTM Standards*, Vol. 04-02, ASTM, West Conshohocken, PA.

[3] Alver, D., M. Ohtsu, and H. Wiggenhauser, Dynamic boundary element method analysis for correction factor determination in impact-echo, *Journal of Transportation Research Board*, Vol. **2050**, 2008, pp. 122-126.

[4] Ryden N. and C.B. Park, A combined multichannel impact echo and surface wave analysis scheme for non-destructive thickness and stiffness evaluation of concrete slabs. *AS NT, 2006 NDE Conference on Civil Engineering*, St. Louis, MO, 2006.

[5] Barnes, C.L. and J.F. Trottier. Hybrid analysis of surface wavefield data from Portland cement and asphalt concrete plates, *NDT&E International*, **42**, 2009, 106-112.

[6] Alggernon, D., Impact-echo data analysis based on duration and bandwidth of the signal components, *Journal of Transportation Research Board*, **2050**, 2008, pp. 127-133.

[7] Huang, N.E., S. Zheng, S.R. Long, M.C. Wu, H,H. Shih, Q. Zheng, N-C. Yen, C.C. Tung, and M.H. Liu. The empirical mode decomposition and Hilbert spectrum for nonlinear and nonstationary time series analysis. *Proceedings of Royal Society of London, A* 454, 1998, 903-995.

[8] Huang, N.E., Z. Shen, and R.S. Long, A new view of nonlinear water waves--Hilbert Spectrum, *Ann. Rev. Fluid Mech*. 31, 1999, 417-457.

[9] Flandrin, P., G. Rilling and P. Goncalves, EMD equivalent filter banks, from interpretation to applications, H*ilbert-Huang Transform: Introduction and Applications*, eds. N.E Huang and S.S.P. Shen, World Scientific, Singapore, 2005, 67-87.

[10] Huang, N. and Wu, Z, A review on Hilbert-Huang transform: Method and its applications to geophysical studies, *Reviews of Geophysics*, **46**, RG2006, 2008, 23 pages.

[11] Attoh-Okine, N., K. Barner, D. Bentil, and R. Zhang (Eds) Special issue on The Empirical Mode Decomposition and the Hilbert-Huang Transform, *EURASIP Journal on Advances in Signal Processing*, **2008**, 124 pages, 13 papers.

[12] Zhang, R., S. Ma, E. Safak, and S. Hartzell, Hilbert-Huang transform analysis of dynamic and earthquake motion recordings, *ASCE Journal of Engineering Mechanics,* **129**, 8, 2003, pp 861-875.

[13] Zhang, R. and L.D. Olson, Dynamic bridge substructure condition assessment with Hilbert-Huang Transformation – Simulated flood and earthquake damage to monitor structural health and security," *TRB, Journal of the Transportation Research Board*, **1892**, 2004, 153-159.

[14] Zhang, R., R. King, L. D. Olson and Y.L. Xu, Dynamic response of the Trinity River Relief bridge to controlled pile damage: modeling and experimental data analysis comparing Fourier and Hilbert-Huang techniques, *Journal of Sound and Vibration*, **285**, 2005, 1049-1070.

[15] Zhang, R. Characterizing and quantifying earthquake-induced site nonlinearity, *Soil Dynamics and Earthquake Engineering*, **26**, 2006, 799-812.

[16] Zhang, R., A simple approach for quality evaluation of non-slender, cast-in-place piles, *Smart Structures & Systems*, **4**, 2008, 1-15.

[17] Zhang, R, A recording-based approach for identifying seismic site liquefaction and nonlinearity via HHT data analysis, *Advances in Adaptive Data Analysis*, **1**, 2009, 89-123.

[18] Wu, Z. and N. Huang, Ensemble empirical mode decomposition: a noise-assisted data analysis method, *Advances in Adaptive Data Analysis*, **1**, 2009, 1-41.